

Enhanced Decoupled Disturbance Observer for Dual-Stage Hard Disk Drives

Shiyong Zhou, Xu Chen and Masayoshi Tomizuka

Department of Mechanical Engineering

University of California, Berkeley

December 2014

Executive Summary

This report presents handling of repetitive disturbances in the dual-stage hard disk drives. The decoupled sensitivity design provides the basic framework. The baseline controllers for voice coil motor(VCM) and Lead (Pb) Zirconium Titanate (PZT) loops are designed by discrete Linear Quadratic Gaussian/ Loop Transfer Recovery (LQG/LTR). Then two enhanced Repetitive Disturbance Observer(RDOB) are added to the dual stage structure separately for periodic disturbances rejection. Selective band Q filter is designed separately for the VCM and PZT loops' RDOB so that VCM can work mainly in low frequency (0 – 1000Hz) range and PZT works in the middle (1000Hz – 2000Hz) frequency range to avoid saturation. The proposed design is evaluated by simulation.

Contents

1	Introduction	3
2	HDD plant models and Decoupled sensitivity design of dual-stage servo	4
3	Baseline control design by discrete LQG/LTR	7
3.1	Introduction to Discrete Linear Quadratic Gaussian/ Loop Transfer Recovery(LQG/LTR)	7
3.2	Design details about Discrete LQG/LTR design in dual stage decoupled sensitivity structure	9
3.3	Baseline controller design result by Discrete LQG/LTR	11
4	Disturbance observer(DOB) and enhanced repetitive disturbance observer(RDOB)	12
4.1	Introduction to discrete disturbance observer(DOB) and repetitive disturbance observer(RDOB)	12
4.2	Enhanced repetitive disturbance observer on dual stage HDD servo	15
4.3	Design of Q filter	16
5	Simulation results	17
6	Conclusion	19
6.1	Conclusion of current work	19
6.2	Future work	19

1 Introduction

Hard Disk Drives(HDDs) are the most commonly used data storage devices nowadays. The control tasks in HDDs are categorized into two types. One is referred to as track seeking and the other is track following. Track following requires that the Read/Write head can follow the center of the data track as precisely as possible in presence of different kinds of disturbance. Due to increasing data storage density, the control requirements in HDD track following are becoming more and more stringent. The conventional single stage HDD control scheme by using voice coil motor (VCM) is no longer able to satisfy the requirements because of its limited achievable bandwidth. So a second actuator is introduced to complement the single actuation scheme. The Lead (Pb) Zirconium Titanate (PZT) dual stage actuation is one of the techniques by re-designing the suspension to accommodate an active component made from piezoelectric material. As a result, the control scheme becomes a dual-input-single-output (DISO) system. Various control design architectures have been proposed for this dual-stage servo structure (see ref [4]), which can be mainly classified into two categories. One is based on the classical single-input-single-output (SISO) design technique by properly design observers to decouple the control loop. Examples are master-slave(Koganezawa et al., 1999) and decoupled sensitivity design approaches (Mori et al., 1991) , the PQ method (Schroeck et al., 1999) and a direct parallel design approaches. The other is based on modern state-space-based MIMO control methodologies. Examples are optimal and robust control techniques like LQG/LTR , H-infinity and u-synthesis and so on (Suzuki et al., 1997; Hu et al., 1999; Hernandez et al., 1999).

Besides, HDDs are subjected to periodic disturbances caused by either internal components of the drive or sources external to the HDD. The periodic disturbance will have definite temporal pattern and they remain the same every time the disks are spun. This causes the so-called repeatable runout (RRO) during the track following controller's operation. Repetitive control (RC) (see [8]) is a well-known servo design tool for systems that are subjected to periodic disturbances/reference. An internal model $\frac{1}{1-z^{-N}}$ (N is the period of the disturbance/reference) is incorporated into the feedback system such that errors in previous repetition can be used to improve the current tracking or regulation performance. However, RRO signal is on top of the non-repeatable runout (NRRO) present in the head-disk assembly and spindle-disk assembly. When the conventional RC is used, due to limitations from Bode's Integral Theorem, the improvement in repetitive frequencies will come along with degradation in other frequencies which may include NRRO.

So in order to extend the bandwidth of single stage HDDs and at the same time address the repetitive disturbance present in HDD without sacrifice of performance in other non-repetitive frequencies, discrete time LQG/LTR design (ref [5]) for dual stage HDDs track following control with decoupled sensitivity design is used for faster loopshaping of the fundamental control frame. Besides, the enhanced repetitive disturbance observer (ref [3]) is design as an add-on feature on the dual-stage control structure to address the repetitive disturbance in low(0-2000Hz) and high frequency(2000-5000Hz) range.

This report is organized as follows.

- Section 2: HDD plant models and Decoupled sensitivity design of dual-stage servo

- Section 3: Baseline control design by discrete LQG/LTR
- Section 4: Disturbance observer(DOB) and enhanced repetitive disturbance observer(RDOB)
- Section 5: Simulation results
- Section 6: Conclusion

2 HDD plant models and Decoupled sensitivity design of dual-stage servo

Hard Disk Drive(HDD) is used for massive media data storage extensively nowadays. Data in an HDD are arranged in concentric circles or tracks and are read or written with a read/write (R/W) head. The two main functions of the head positioning servomechanism in disk drives are track seeking and track following. Track seeking moves the R/W head from the present track to a specified destination track in minimum time using a bounded control effort. Track following maintains the head as close as possible to the destination track center while information is being read from or written to the disk. So the control task for track following requires high accuracy and good disturbance rejection in high bandwidth while the control task for track seeking requires short-span track seek with smooth and fast settling. The R/W head is actuated by Voice Coil Motor (VCM) in single stage HDDs. However, with the ever increasing demand for larger storage capacity in HDDs, piezoelectric-based (PZT) dual-stage actuator has been added to the single stage VCM actuator to break the bottleneck of the single-actuator HDDs and some research on dual-stage HDD emerge, such as [2]. In this enhanced mechanical structure, a micro-actuator is mounted on a conventional VCM actuator for accurate positioning of the Read/Write head which is attached to the end of the MA, as shown in Figure 1. In this so-called dual stage scenario, the VCM provides coarse motion for the position servo depending on its wide range of motion while the added PZT actuator provides faster and finer positioning due to its limited range of motion.

Another consideration for the controller design in dual stage HDDs is that, even though in the dual-stage HDDs, the VCM and PZT are actuated together to generate the motion of the Read/Write head, the only available measurement is the displacement of the Read/Write head slider from embedded servo sector pattern on the surface of the HDDs. So the controller design problem for the dual-stage HDDs becomes a control problem for a dual-input single-output (DISO) system. If the relative displacement of the secondary stage actuator with respect to the VCM can be somehow measured or estimated, the design for the DISO system will become easier and makes the controller design for the VCM and PZT loop separately. Several structures in literature have been proposed to simplified the design challenge for the dual-stage HDDs [6].

As mentioned before, a practical model for VCM in dual-stage HDD plant can be of more than twenty orders, as shown in Figure2 from HDD benchmark package. The full model of VCM used for Discrete LQG/LTR design is a double integrator with several resonance modes. And the full model for PZT is a pure gain with two resonance mode which are at the same frequencies as for

those for VCM. The transfer function for the VCM and PZT are expressed in the form below:

$$G_{vcm}(s) = \frac{K_V}{s^2} + \sum_{i=1}^5 \frac{g_{vi}w_{vi}^2}{s^2 + 2\zeta_{vi}w_{vi}s + w_{vi}^2} \quad (1)$$

$$G_{pzt}(s) = K_p + \sum_{i=1}^2 \frac{g_{pi}w_{pi}^2}{s^2 + 2\zeta_{pi}w_{pi}s + w_{pi}^2} \quad (2)$$

The parameter for the resonance modes are shown in Table. 1.

High frequency resonances are usually attenuated by notch filters which can be designed intuitively. Considering the fact that it is very difficult to direct design controller using discrete LQG/LTR based on such high-order model, during Discrete LQG/LTR design , a nominal model which captures the central frequency properties can be considered as the control plant. For the VCM loop, the lower-order model captures the central frequency properties can be described as

$$\begin{bmatrix} x_{v1}(k+1) \\ x_{v2}(k+1) \end{bmatrix} = A_v \begin{bmatrix} x_{v1}(k) \\ x_{v2}(k) \end{bmatrix} + B_v u_v \quad (3)$$

where u_v is the VCM actuator input, x_{v1} is the position of the VCM head in the unit of tracks, x_{v2} is the velocity, and

$$\begin{aligned} A &= \begin{bmatrix} 1 & T \\ 0 & 1 \end{bmatrix} \\ B &= \begin{bmatrix} T^2 k_y k_v \\ T k_y k_v \end{bmatrix} \end{aligned} \quad (4)$$

T is the sampling time, k_v is the acceleration constant, and k_y is the position measurement gain. For the PZT loop, the nominal model is a pure gain and can be described as follow:

$$x_m(k+1) = 0x_m(k) + K_m u_m \quad (5)$$

where x_m is the position of PZT head in the units of track. K_m is a constant gain which is determined by the plant. u_m is the control signal for the PZT loop. The overall output of the system is the overall position of VCM loop plus PZT loop, as described as follow:

$$y(k) = y_v(k) + y_m(k) = C_v x_v(k) + C_m x_m(k) \quad (6)$$

The system parameters are set as follows:

rotation speed = 7200rpm

the number of servo sector = 220

the sampling time: $T = 3.7879 \times 10^{-5} sec$

the acceleration constant $k_v = 951.2 \frac{m}{(s^2 A)}$

the position measurement gain $k_y = 3.937 \times 10^6 track \cdot m^{-1}$

The bode diagram of the simplified nominal model is described in Figure 2.

One consideration for the controller design in dual stage HDDs is that, even though in the dual-stage HDDs, the VCM and PZT are actuated together to generate the motion of the Read/Write head, the only available measurement is the displacement of the Read/Write head slider from embedded servo sector pattern on the surface of the HDDs. So the controller design problem for the dual-stage HDDs becomes a control problem for a dual-input single-output (DISO) system. If the relative displacement of the secondary stage actuator with respect to the VCM can be somehow measured or estimated, the design for the DISO system will become easier and makes the controller design for the VCM and PZT loop separately. The decoupled sensitivity design in Figure 3 is one of the simple methods to allow for separated controller design. The open loop transfer function for the structure can be derived as

$$C_v P_v + C_v P_v \hat{P}_m C_m + C_m P_m \quad (7)$$

So the sensitivity function is

$$\frac{1}{(1 + C_v P_v)(1 + C_m P_m) + C_v P_v C_m (\hat{P}_m - P_m)} \quad (8)$$

$$\approx \frac{1}{(1 + C_v P_v)(1 + C_m P_m)}$$

Note that, to guarantee the approximation above, at low frequency range, $P_m = \hat{P}_m$, at high frequency range, since the loop shape of $C_v P_v$ will be designed to roll off at high frequencies, the term $C_v P_v C_m (\hat{P}_m - P_m)$ will also be small, so the approximation is guaranteed. Thus as long as the individual controller for VCM and PZT loop are stable and proper-designed, the overall stability can be guaranteed.

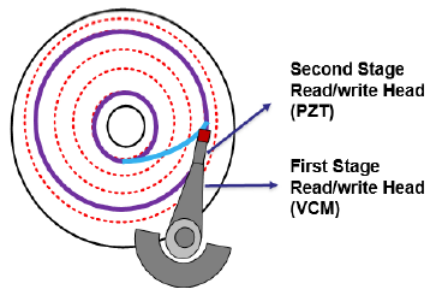


Figure 1: Actuators on dual-stage HDDs

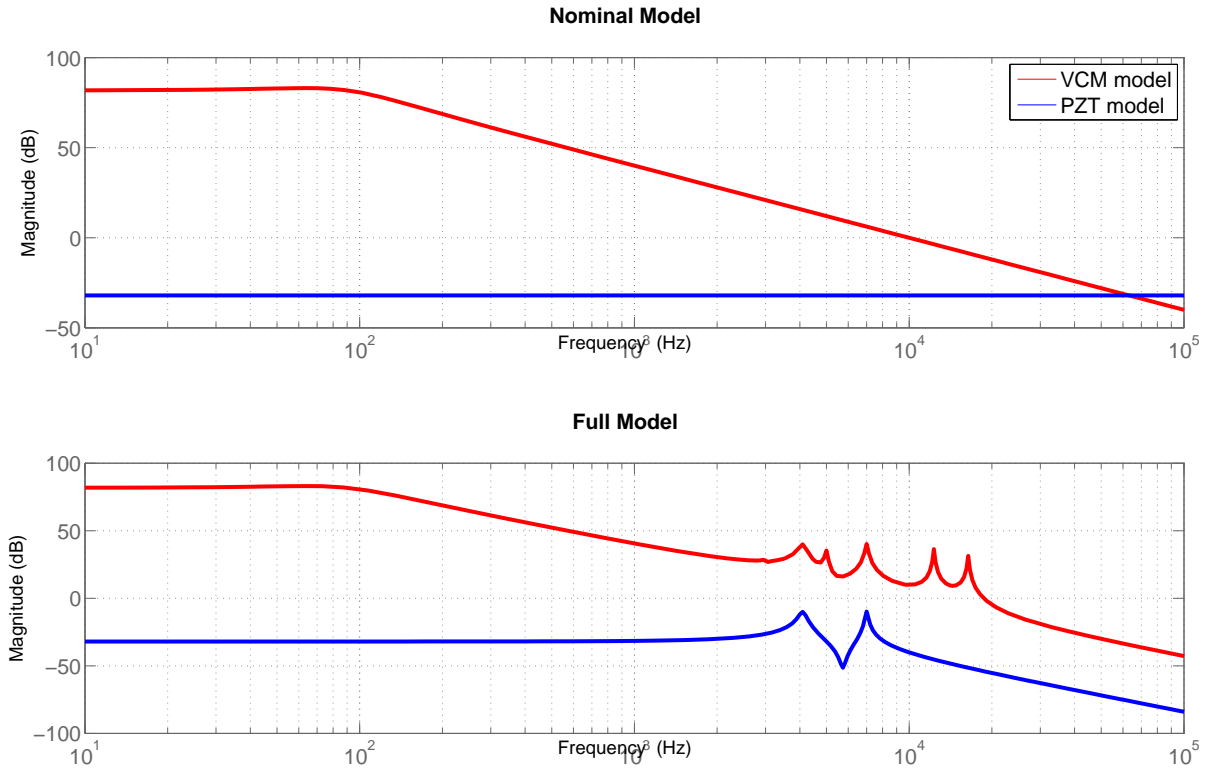


Figure 2: bode plot for nominal and full model of dual stage HDD

3 Baseline control design by discrete LQG/LTR

3.1 Introduction to Discrete Linear Quadratic Gaussian/ Loop Transfer Recovery(LQG/LTR)

The linear quadratic (LQ) optimal control theory ensures the asymptotically stability and attractive robustness property of the optimal state feedback system under controllability and observability (stabilizability and detectability) assumptions. Besides, the steady state Kalman Filter provides an asymptotically stable stochastic state observer. The LQG method combines the optimal state feedback controller and the least square Kalman Filter when there is noise in the control system. However, when state estimator is included, the nice properties of either LQ systems or Kalman filters are lost. In order to exploit the design benefit in LQ controller and Kalman filter (since when regulation matrix (Q,R) and noise covariance (W,V) are specified, the controllers and estimators can be machine computed), the loop transfer recovery (LTR) is introduced for its usefulness in the sense of design.

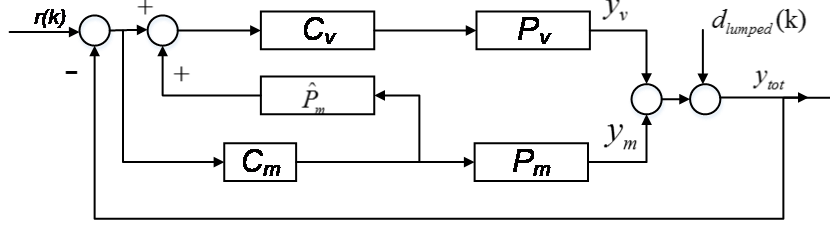


Figure 3: Decoupled sensitivity of dual stage HDDs

modes	1	2	3	4	5
VCM response					
Frequency[Hz]	4100	5000	7000	12300	16400
Damping ratio	0.03	0.01	0.01	0.005	0.005
Gain	-1	0.3	-1	1	-1
PZT response					
Frequency[Hz]	4100		7000		
Damping ratio	0.03		0.01		
Gain	1		1		

Table 1: Parameter comparison

The loop transfer recovery methodology for the linear quadratic gaussian problem is called LQG/LTR. It allows the excellent robustness and sensitivity properties of the optimal state feedback schemes to be almost recovered by the output feedback schemes. This method simplifies the use of the LQG methodology and allows the practical feedback design to be attained with a reasonable amount of effort. The asymptotic recovery approach requires only one pair of the cost weighting matrix or noise covariance matrix to be designed and the other pair is automatically assigned during the recovery process. This results in a tremendous reduction in the complexity of the design process. While the continuous time LQG/LTR exists, this report utilizes the Discrete LQG/LTR method for the design of the baseline controller. The mechanism by which the recovery is achieved is essentially the same as in the continuous time case: the compensator cancels the plant zeros and possibly some of the stable poles, and inserts the controller (observer) zeros. So this will fail if the plant has zeros outside the unit circle, since the compensator guarantees internal stability. The main theorem for the recovery result is as follows:

Theorem 1. *If the open loop transfer function for the system (13) has no finite zero in $\{z : |z| > 1\}$ and $\det(CB) \neq 0$, then*

$$\lim_{R \rightarrow 0} G_p G_{LQG} = G_{TFL} \quad (9)$$

where $G_p = C(zI - A)^{-1}B$ is the open loop transfer function from control to output, and G_{LQG} is the LQG controller specified in (21) and G_{TFL} is the target feedback loop specified in (16).

3.2 Design details about Discrete LQG/LTR design in dual stage decoupled sensitivity structure

Utilizing the fact that the VCM loop and PZT loop can be decoupled in sensitivity function, so the design of VCM and PZT controller can be separated. Therefore, single-input-single-output(SISO) discrete LQG/LTR is intuitive and can be customized for the individual VCM and PZT loop controller design easily. Since the design steps using discrete LQG/LTR will be the same for VCM and PZT loop, only the process for VCM controller design will be illustrated below. Note that, an enhanced repetitive disturbance observer(RDOB) will be incorporated into the servo so as to improve the RRO compensation performance.

1. Decide the state space model for VCM plant which is

$$\begin{aligned} x_v(k+1) &= A_v x_v(k) + B_v u_v(k) \\ y_v(k) &= C_v x_v(k) \end{aligned} \quad (10)$$

Incorporate the desired controller property, which is a single integrator in this case:

$$u_v = \frac{Tz}{z-1} u \quad (11)$$

where u is the real control input. So the overall design plant model(DPM) is

$$\begin{aligned} \begin{bmatrix} x_v(k+1) \\ x_c(k+1) \end{bmatrix} &= \begin{bmatrix} A_v & B_v C_c \\ 0 & A_c \end{bmatrix} \begin{bmatrix} x_v(k) \\ x_c(k) \end{bmatrix} + \begin{bmatrix} B_v D_c \\ B_c \end{bmatrix} u(k) \\ y_v(k) &= [C_v \quad 0] \begin{bmatrix} x_v(k) \\ x_c(k) \end{bmatrix} \end{aligned} \quad (12)$$

where subscript c denotes the model realization from real control input u to desired control u_v . A,B,C represent the corresponding state matrix.

2. Discrete time steady state Kalman Filter Design. Denote $x_e = \begin{bmatrix} x_v \\ x_c \end{bmatrix}$

The augmented system with input noise $w(k)$ and output noise $v(k)$ is

$$\begin{aligned} x_e(k+1) &= A_e x_e(k) + B_e u(k) + Lw(k) \\ y_e(k) &= C_e x_e(k) + v(k) \end{aligned} \quad (13)$$

where $E(w(k)w^T(k)) = 1$ and $E(v(k)v^T(k)) = \mu$. L and μ are two design parameters in Discrete LQG/LTR design. By choosing L and μ properly ($L = B$ normally) and solve the discrete algebraic Reccati equation (DARE) below

$$M = A_e M A_e^T - A_e M C_e^T (C_e M C_e^T + \mu)^{-1} C_e M A_e^T + L L^T \quad (14)$$

The Kalman filter gain can be obtained as

$$F = M C_e^T (C_e M C_e^T + \mu)^{-1} \quad (15)$$

So the target feedback loop we want to recover is

$$G_{TFL} = C_e (zI - A_e)^{-1} A_e F \quad (16)$$

3. Solve the discrete time ‘cheap’ control problem where the cost function is

$$J = \frac{1}{2} \sum_k \{x^T(k)Qx(k) + Ru^2(k)\} \quad (17)$$

$$Q = C^T C$$

The DARE for the ‘cheap’ control problem will be

$$P = A^T P A + Q - A^T P B (R + B^T P B)^{-1} B^T P A \quad (18)$$

so the feedback gain will be

$$K = -(R + B^T P B)^{-1} B^T P A \quad (19)$$

In summary, the Discrete LQG/LTR controller will be

$$G_{LQG} = zK \{zI - (I - FC_e)(A_e - LK)\}^{-1} F \quad (20)$$

The proof for this in Proposition. 1.

Proposition 1. *The discrete LQG/LTR controller for design plant model as*

$$x_e(k+1) = A_e x_e(k) + B_e u(k)$$

$$y_e(k) = C_e x_e(k)$$

can be written as

$$G_{LQG} = zK \{zI - (I - FC_e)(A_e - LK)\}^{-1} F \quad (21)$$

Proof. The state space representation for the Discrete LQG will be

$$u(k) = -K \hat{x}(k|k) \quad (22)$$

$$\hat{x}(k+1|k+1) = A \hat{x}(k|k) + Bu(k) + F(k+1)[y(k+1) - CA \hat{x}(k|k) - CBu(k)] \quad (23)$$

Substitute equation 22 into 23, the transfer function from $y(k+1)$ to $u(k)$ can be obtained as

$$G_{y(k+1) \rightarrow u(k)} = K[zI - (A_e - LK) - FC(A_e - LK)]^{-1} F \quad (24)$$

Then advance for one step results in the transfer function from $y(k)$ to $u(k)$. So the final transfer function is equation 21. \square

Remark 1. *If it is impossible or not a good choice to use $\hat{x}(k|k)$, one can instead use $\hat{x}(k|k-1)$ for the control implementation, then the LQG/LTR controller will become*

$$G_{LQG} = K(I - FC)[zI - (A - BK)(I - FC)]^{-1}(A - BK)F + KF \quad (25)$$

where A, B, C are corresponding state space matrix of the design plant model. The control action is expressed as

$$u(k) = -K \hat{x}(k|k-1) \quad (26)$$

Details can be seen in references [1], [5] and [7].

	Gain Margin(dB)	GM Frequency(Hz)	Phase Margin (Degree)	PM Frequency(Hz)
VCM	4.2766	4386	69.85	982
PZT	9.0726	13199	119.2927	1156.5

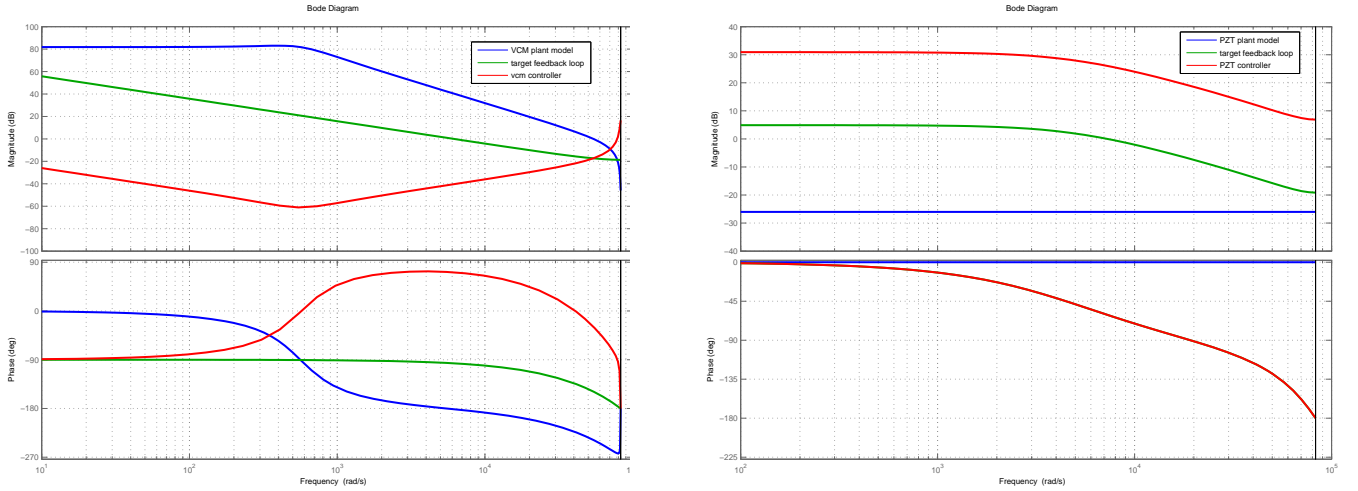
Table 2: Gain margin and phase margin for vcm loop and pzt loop

3.3 Baseline controller design result by Discrete LQG/LTR

A integrator is included in the vcm desired controller for extra disturbance regulation at low frequency, and L is chosen as B_e . The noise parameter $\mu = 10^8$, then the cheap control $R = 1e^{-13}$. The final controller is the recovered control in series with the integrator. A gain $k = 5000$ is added to the final controller for bandwidth extension. The final result can be seen in Fig 4a. The gain margin can phase margin parameter is shown in Table 2.

For the PZT loop, the nominal model is just a pure gain, so a lag compensator is initialized at first in the desired controller effort, then the LTR is carried out with $L = B_e$ and $\mu = 5e^{-5}$ and $R = 2e^{-4}$. Likewise, an extra gain $k = 20$ is added to the controller. Note that due to the pure gain property of PZT plant, this LQG/LTR procedure is actually just automatically tuning a proper loop shape for the PZT loop and the tuning parameter is actually the two turning frequencies of the lag compensator at the first step. The result can be sen in Figure 4b with the gain margin and phase margin in 2.

The individual sensitivity and overall sensitivity for the dual stage HDDs in shown in Figure 5.



(a) LTR result for vcm loop

(b) LTR result for pzt loop

Figure 4: the LQG/LTR result for vcm and pzt loop

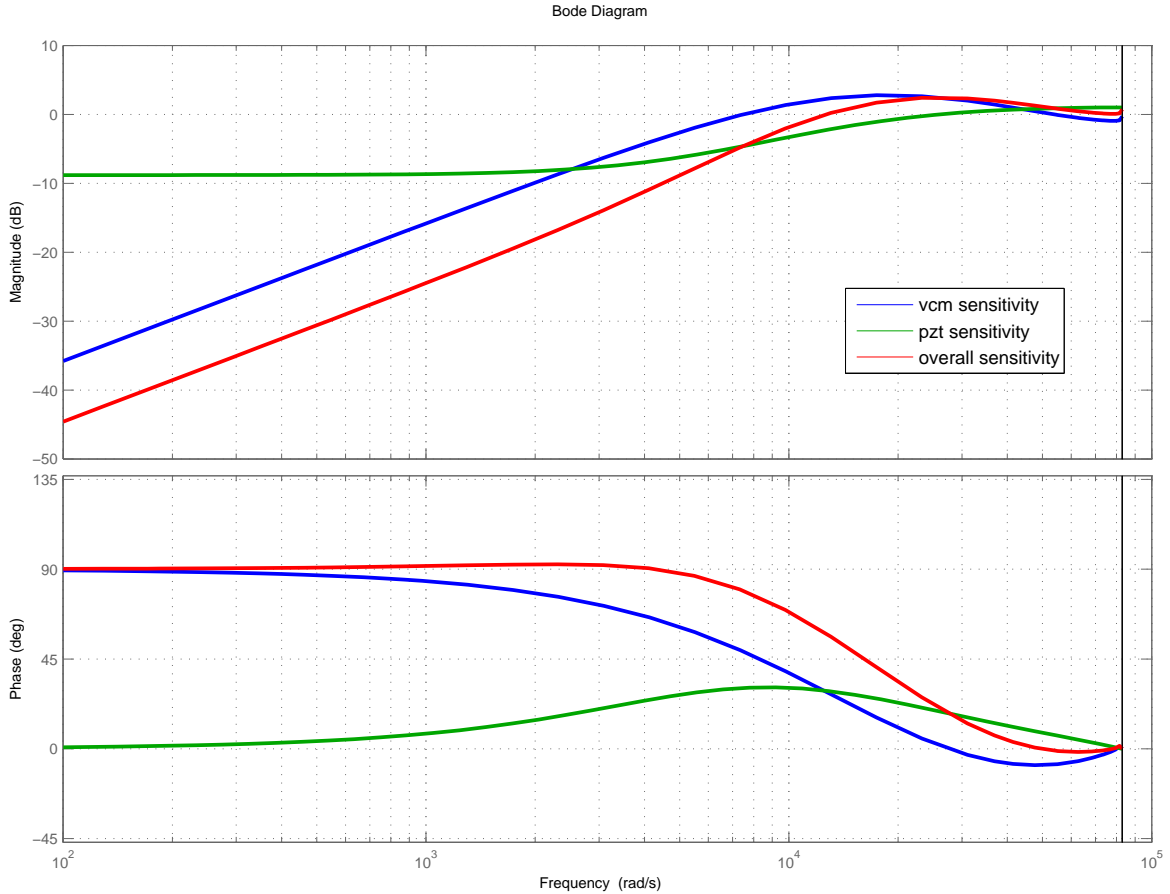


Figure 5: sensitivity function for vcm and pzt loop and overall sensitivity

4 Disturbance observer(DOB) and enhanced repetitive disturbance observer(RDOB)

4.1 Introduction to discrete disturbance observer(DOB) and repetitive disturbance observer(RDOB)

In control of mechanical system, uncertainties exist like friction, varying load inertia, ignored dynamics, actuator saturation, backlash, sensor noise and so on. There are several ways to handle uncertainties. They can be classified into two categories: robust control and adaptive control. Popular robust control techniques include sliding mode control, H_∞ control and disturbance observer.

Disturbance Observer is a clever approach for handling disturbance in motion control. It is introduced by Ohnishi(1987) (Murakami and Ohnishi (1990)) and refined by Umeno and Hori(1991). The discrete time version of disturbance observer is shown in Figure 7. To understand this structure, note that the signal coming into the Q filter is essentially delayed disturbance signal and some model mismatch between $P(z^{-1})$ and $z^{-m}P_n(z^{-1})$. So after proper Q filtering, we can remove the unwanted By rearranging the blocks, the structure in Figure 7 can be modified into the one in Figure 8, so it can be seen clearly that the transfer function from $d(k)$ to $y(k)$ is

$$\begin{aligned} G_{d(k) \rightarrow y(k)}(z^{-1}) &= \frac{P(z^{-1})}{1 + \frac{1}{1-z^{-m}Q(z^{-1})} \frac{Q(z^{-1})}{P_n(z^{-1})} P(z^{-1})} \\ &= \frac{(1 - z^{-m}Q(z^{-1}))P(z^{-1})P_n(z^{-1})}{(1 - z^{-m}Q(z^{-1}))P_n(z^{-1}) + Q(z^{-1})P(z^{-1})} \\ &\approx (1 - z^{-m}Q(z^{-1}))P(z^{-1}) \end{aligned} \quad (27)$$

So by designing $Q(z^{-1})$ properly, the desired dynamics can be incorporated into the plant.

Recall that the sensitivity function for linear feedback control systems is $\frac{1}{1+G_{open}(s)}$, so a high gain nature is expected in robust control systems for good performance. Repetitive control(RC) is a good example of exploiting the idea of high gain control. It sets the open loop gain to infinity or a large value at known frequencies of periodic disturbance by absorbing the internal model $\frac{1}{1-z^{-N}}$ into the open-loop transfer function. However, due to limitations from Bode's Integral Theorem, the comb-shape peaks in magnitude response of open loop transfer function created by this internal model is not narrow as a result that disturbance in non-repetitive frequencies are amplified. Examples can be seen in Figure 6. This problem becomes more severe if there are large non-periodic components in the disturbance. Therefore, a modified version of the internal model of periodic disturbance is proposed in [3] with an embedded tuning parameter α . As a result, the amplification can be adjusted by the tuning parameter α . Combine with (27), if the Q filter can be designed as

$$1 - z^{-m}Q(z^{-1}) = \frac{1 - z^{-N}}{1 - \alpha^N z^{-N}} \quad (28)$$

Then considering the complete feedback system with DOB in Figure 9. if the reference signal is zero(for regulation purpose), then the bloc diagram can be recast into the one shown in 10. Denote the transfer function from $e(k)$ to $u(k)$ as $C_{eq}(z^{-1})$ (equivalent controller), then the transfer function is

$$\begin{aligned} C_{eq}(z^{-1}) &= \frac{C(z^{-1}) + Q(z^{-1})P_n^{-1}(z^{-1})}{1 - z^{-m}Q(z^{-1})} \\ &\text{where } \alpha \in [0, 1) \end{aligned} \quad (29)$$

From the structure in 10, we can easily obtain the sensitivity function as

$$\begin{aligned} S(z^{-1}) &= \frac{1}{1 + P(z^{-1})C_{eq}(z^{-1})} \\ &= \frac{1 - z^{-m}Q(z^{-1})}{1 + P(z^{-1})C(z^{-1}) + (PP_n^{-1}(z^{-1}) - z^{-m})Q(z^{-1})} \end{aligned} \quad (30)$$

Therefore, from equation (30), in the frequency range where the plant $P(e^{-j\omega})$ is well modelled by $e^{-jm\omega} P_n(e^{-j\omega})$, we can obtain $PP_n^{-1}(z^{-1}) - z^{-m} \approx 0$, so the sensitivity function in (30) can be rewritten into

$$S(z^{-1}) = \frac{1 - z^{-m}Q(z^{-1})}{1 + P(z^{-1})C(z^{-1})} \quad (31)$$

Assume that the disturbance contains only periodic component that satisfies

$$(1 - z^{-N})d(k) = 0 \quad (32)$$

Then by the design in (29), the periodic disturbance will be attenuated at the repetitive frequencies while the amplification in non-repetitive frequencies can be alleviated by tuning parameter α . Magnitude response corresponds to different α can be seen in Figure 11 which is extracted from reference [3].

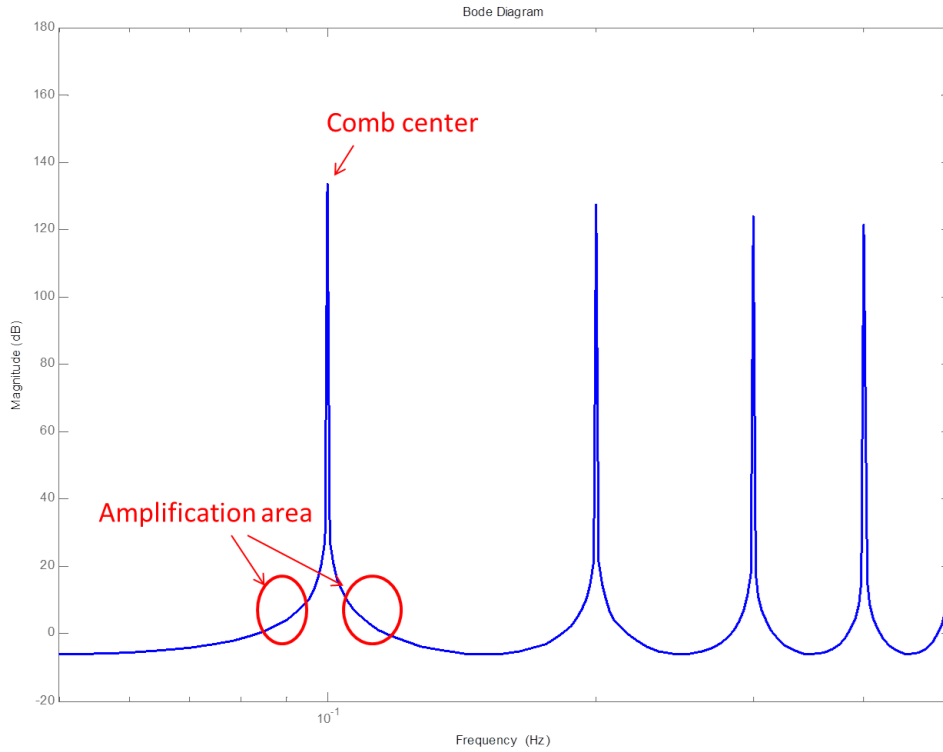


Figure 6: Magnitude response of $\frac{1}{1-z^{-10}}$ with sampling frequency $T_s = 1$. Amplification in frequencies other than comb center can be seen.

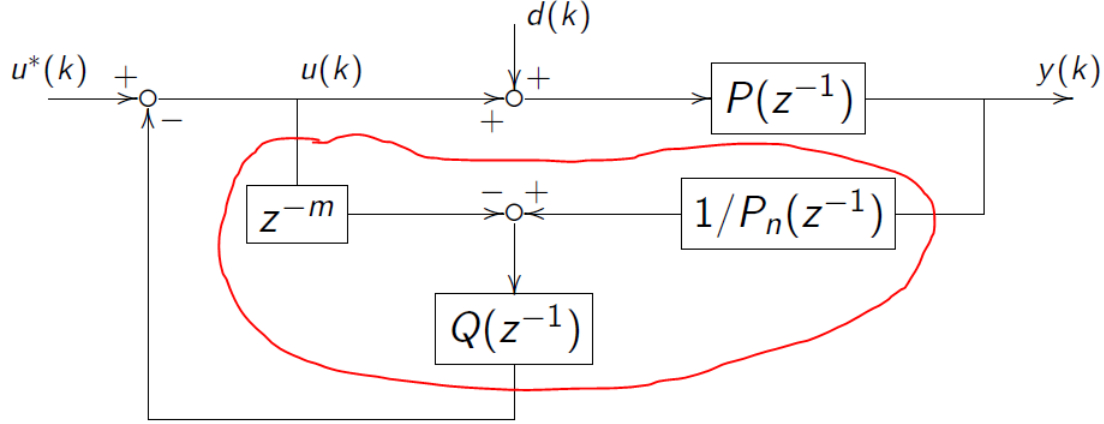


Figure 7: Block diagram of discrete system plant with discrete added-on DOB, the plant model is approximately $P(z^{-1}) \approx z^{-m}P_n(z^{-1})$. The structure in the red curve is the DOB. m is the relative degree of $P(z^{-1})$. The Q filter needs to be designed properly to ensure good servo performance.

4.2 Enhanced repetitive disturbance observer on dual stage HDD servo

Saturation is a big concern in dual stage HDDs. In order to take advantage of the high bandwidth property of the dual stage HDDs while at the same time try to avoid saturation, the VCM loop is designed to handle the low frequency disturbance and the PZT loop is designed to handle the high frequency disturbance. In this repetitive disturbance observer configuration, different frequency range RDOBs can be added onto VCM loop and PZT loop separately. To add RDOB onto VCM loop, note that a gain estimate of the PZT plant is used to estimate the VCM output, then the standard way for estimating disturbance in DOB framework is used. The block diagram can be seen in Figure 12. By proper manipulation, the block diagram can be simplified to Figure 13. Likewise, to add RDOB onto PZT loop, it can be constructed as the one shown in Figure 14.

Recall the sensitivity decoupling result from equation (8), denote the equivalent controller for PZT loop as $C_{m(eq)}$, then according to Figure 14, the sensitivity for PZT loop is

$$\frac{1}{C_{m(eq)}P_m + 1} \quad (33)$$

where the equivalent controller is

$$\frac{C_m + Q_m P_{nm}^{-1}}{1 - z^{-m}Q_m} \quad (34)$$

where Q_m is the Q filter for PZT loop DOB and $P_{nm}^{-1} = z^{-m}P_m^{-1}$. Note that the notation (z^{-1}) will be omitted from now on for simplification. So the sensitivity function for PZT loop will be

$$S_m = \frac{1 - z^{-m}Q_m}{1 + P_m C_m + (P_m P_{nm}^{-1} - z^{-m})Q_m} \quad (35)$$

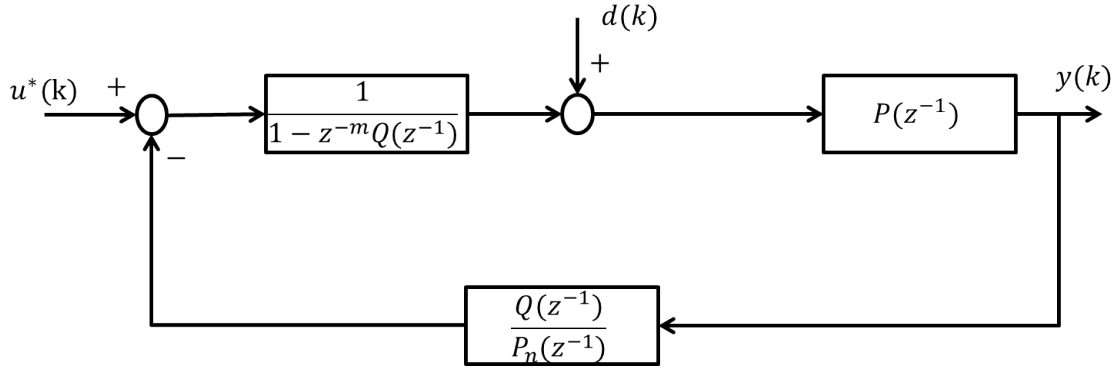


Figure 8: Equivalent diagram of block diagram in 7

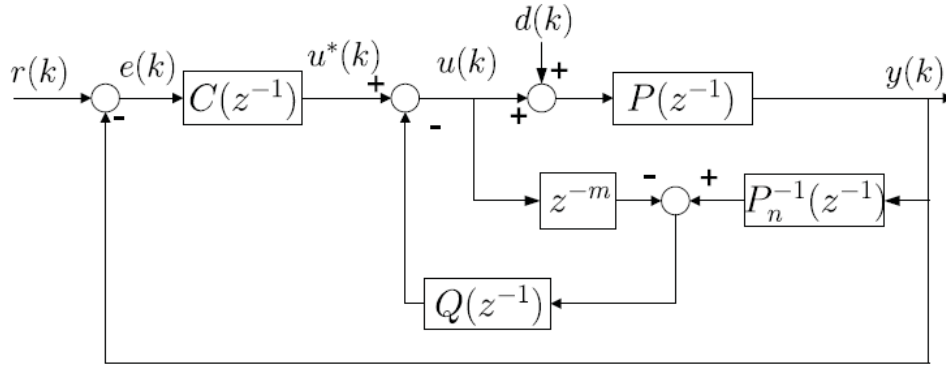


Figure 9: Complete block diagram of a feedback system with add-on DOB

So the factor $1 - z^{-m}Q_m$ is incorporated into the sensitivity of PZT loop which we can then exploit to handle the repetitive disturbance. Note the design procedure for VCM loop RDOB follows. The only difference will be in plant inversion and design of Q filter for handling different frequency band disturbance.

4.3 Design of Q filter

In the previous section, according to the periodic pattern of the DOB, Q filter is designed to be the one in equation 29, so the Q filter can be derived as

$$Q(z^{-1}) = \frac{1 - \alpha^N z^{-(N-m)}}{1 - \alpha^N z^{-N}} \quad (36)$$

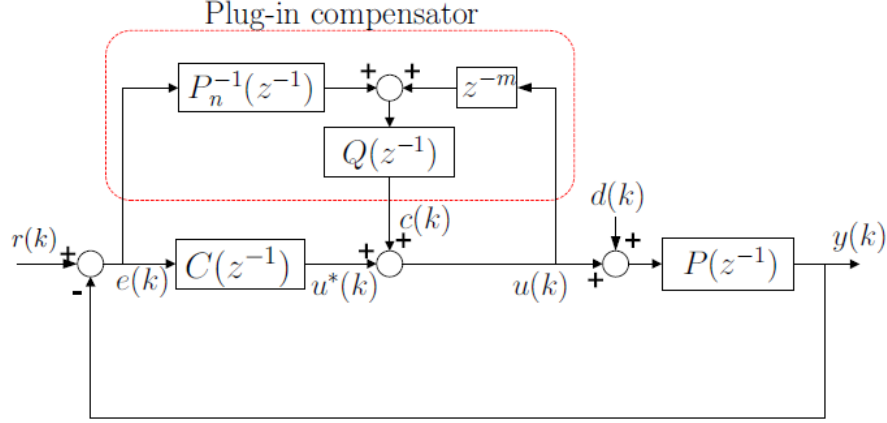


Figure 10: Equivalent block diagram of system in Figure 9

where m is the relative degree of the plant model. Since in the sensitivity function 30, to ensure the approximation of equation (31) is right, one important condition is that $(PP_n^{-1}(z^{-1}) - z^{-m})Q(z^{-1}) \approx 0$. Since it is not possible to have a perfect model, so in frequency range where model mismatch is big, $Q(z^{-1})$ should be deigned to make the term small. So a basic lowpass filter should be designed to Q . A zero-phase low pass filter can be used in this context since it won't change the final structure a low by being zero-phase. A choice of the zero-phase low-pass filter is

$$q_0(z, z^{-1}) = \frac{(1 + z^{-1})^{n_0}(1 + z)^{n_0}}{4^{n_0}} \quad (37)$$

Note to ensure causality in implementation, the additional forward steps n_0 can be 'borrowed' from the large delay in Q filter in (36). Besides, we want the RDOB on PZT loop to have selective disturbance rejection only in restricted area to avoid use of PZT in unnecessary frequency range, so an additional zero-phase bandpass filter is designed by butterworth filter. The butterworth filter's magnitude response is maximally flat in the passband and is monotonic in the passband and stopband. The selective band is from $720Hz$ $3600Hz$. If the bandpass filter is designed as $bp(z^{-1})$, then the zero phase butterworth bandpass filter is

$$bp(z, z^{-1}) = bp(z)bp(z^{-1}) \quad (38)$$

The actual filter used in the simulation is

$$bp_{sim}(z, z^{-1}) = \frac{0.07801 - 0.156z^{-2} + 0.07801z^{-4}}{1 - 2.838z^{-1} + 3.165z^{-2} - 1.694z^{-3} + 0.3816z^{-4}} \times \frac{0.07801z^4 - 0.156z^2 + 0.07801}{1 - 2.838z + 3.165z^2 - 1.694z^3 + 0.3816z^4}$$

5 Simulation results

The above framework is simulated in a HDD benchmark simulink model. The sampling frequency is $f_s = 26400Hz$. The repetitive disturbance N is thus $N = \frac{60f_s}{RPM} = 220$. The resulting sensitivity

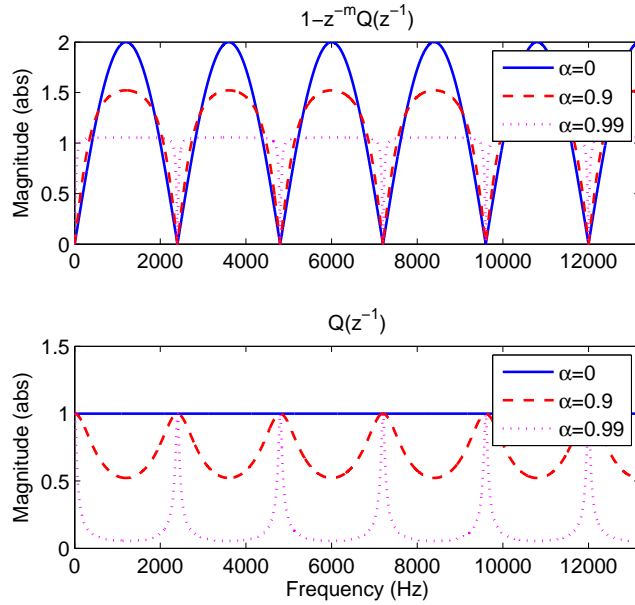


Figure 11: magnitude response of $1 - z^{-m}Q(z^{-1})$ and $Q(z^{-1})$ with different values of α . see ref. [3]

with RDOB is shown in Figure. 15. With the designed selective band Q filter for PZT loop, the sensitivity for PZT loop can be seen from Figure 16.

The compensation results without using RDOB on VCM or PZT loop are shown in figure 17b and figure 18a, from the result, one can see that the dual stage structure improves the overall performance and extends the bandwidth. When the RDOB on VCM loop or PZT loop is enabled, the compensation result is improved. Some important cases are shown in figure. 17 and 18. The frequency $0Hz \sim 2000Hz$ is plotted. One can see that when dual stage and all the RDOBs are turned on, the performance is the best. Besides, when all the disturbance are added to the servo, The enhanced RDOB compensates the repetitive disturbance without sacrificing the performance in non-repetitive frequencies. This is due to the repetitive narrow 'trench' created in the sensitivity function by enhanced RDOB. So the repetitive disturbance is rejected while non-repetitive disturbance is not enhanced so badly due to waterbed effects. As a result, the overall performance are improved with the proposed framework.

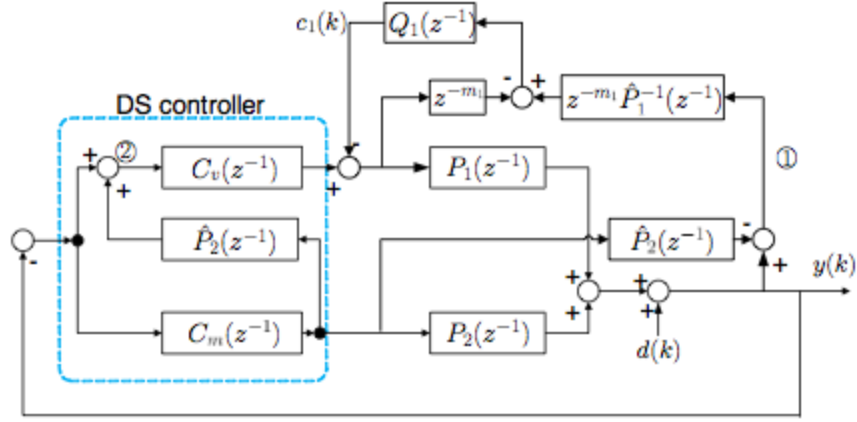


Figure 12: RDOB is added onto VCM loop only.

6 Conclusion

6.1 Conclusion of current work

In this project, the decoupled sensitivity structure for the dual stage HDDs is used as a baseline design framework. Then by taking advantage of the design convenience brought by the decoupled sensitivity structure, the discrete LQG/LTR is used as an efficient design method for the baseline controllers of the VCM loop and PZT loop separately. In order to improve the structure's capability of handling one common disturbance- repetitive disturbance in HDD environment, the enhanced RDOB are incorporated to the VCM loop and PZT loop separately with customized Q filter for specific band disturbance handling. As a result, the VCM RDOB can be used in lower frequency range while the PZT RDOB can be used only in higher frequency range to prevent unnecessary use of PZT in low frequency range. Beside, due to the simple plant model of the PZT plant, the model inversion for the RDOB on PZT loop is easier than that for the VCM plant, so the inclusion of RDOB on PZT loop is easy and efficient. The simulation result validates the proposed framework with improved PES with periodic and non-periodic disturbance.

6.2 Future work

Future works will include designing direct MIMO discrete LQG/LTR controllers for dual stage HDDs to see whether there are other benefits and improvements compared to current framework. The robustness of the structure will also be analyzed. Besides, since the disturbance fundamental frequency may not be known in advance, the adaptive scheme for online disturbance frequency identification will also be investigated.

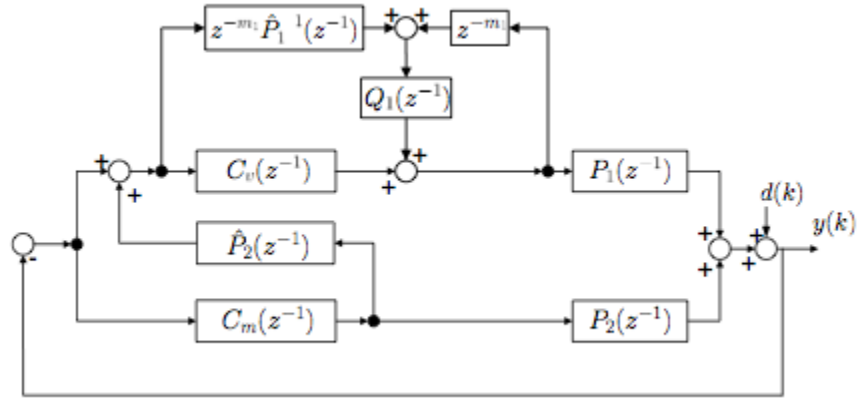


Figure 13: Equivalent block diagram for figure 12

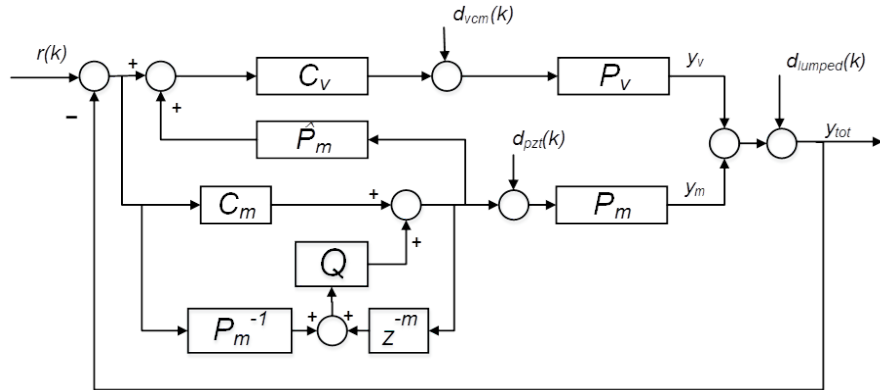


Figure 14: RDOB is added to PZT loop only

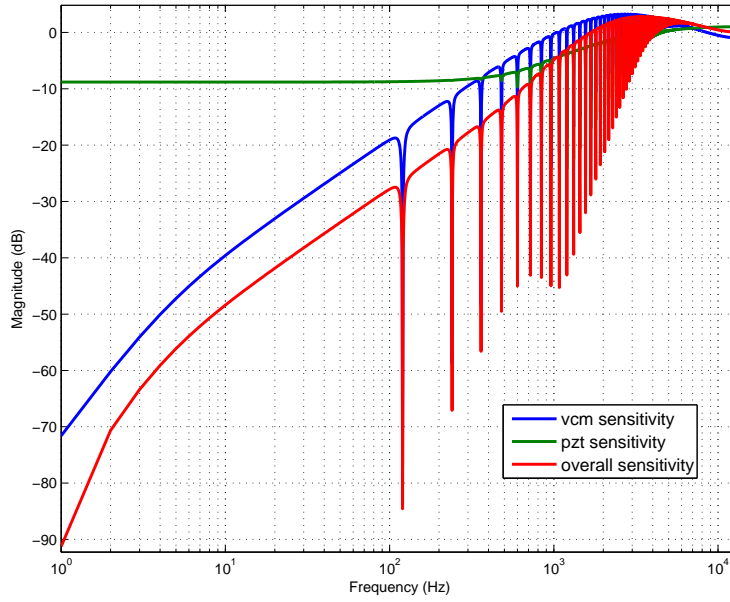


Figure 15: Overall sensitivity function with Discrete LQG/LTR controller and RDOB

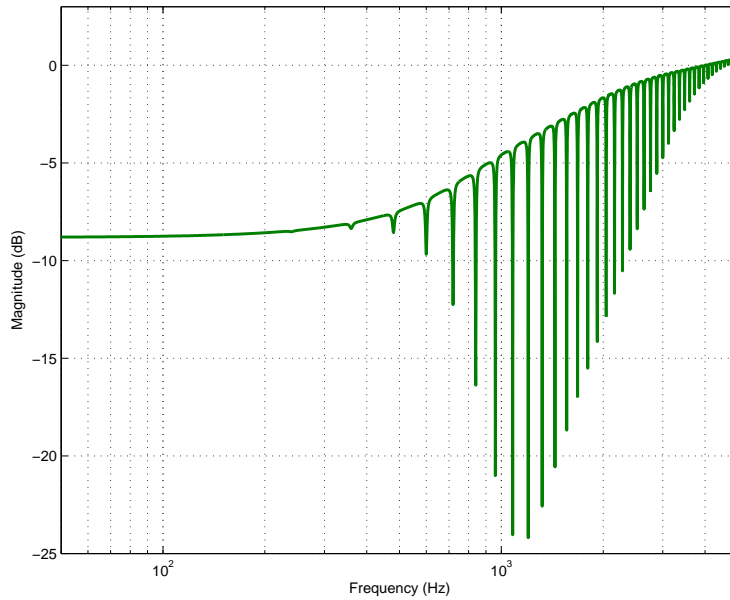
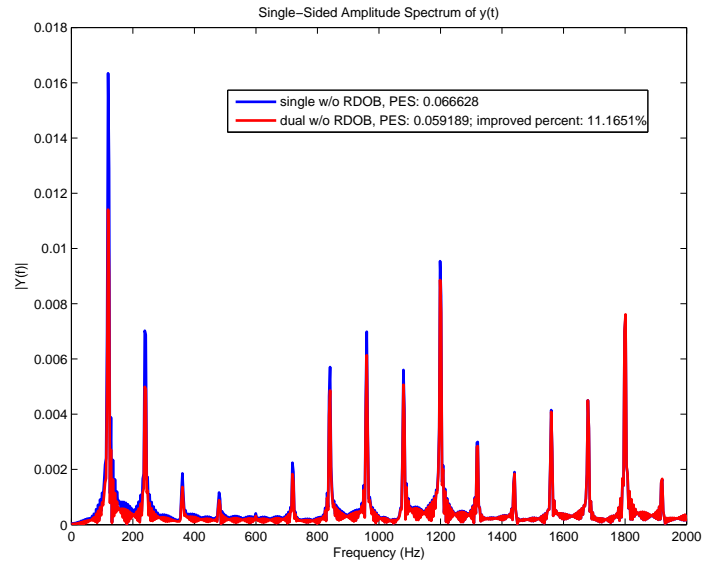
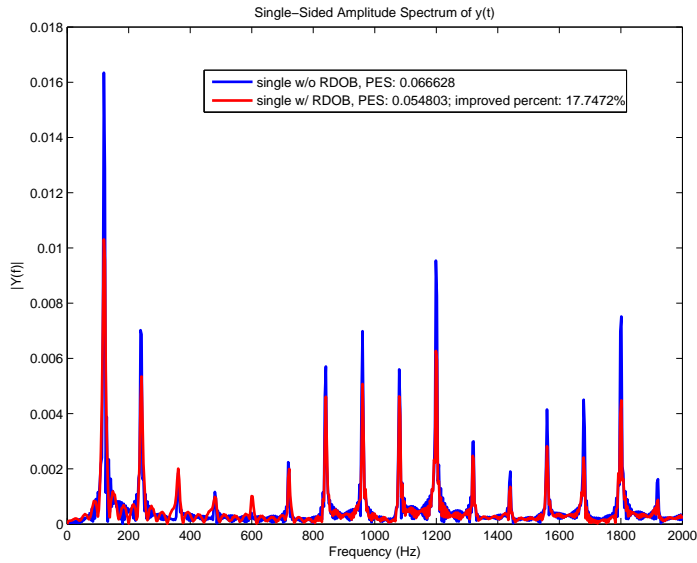
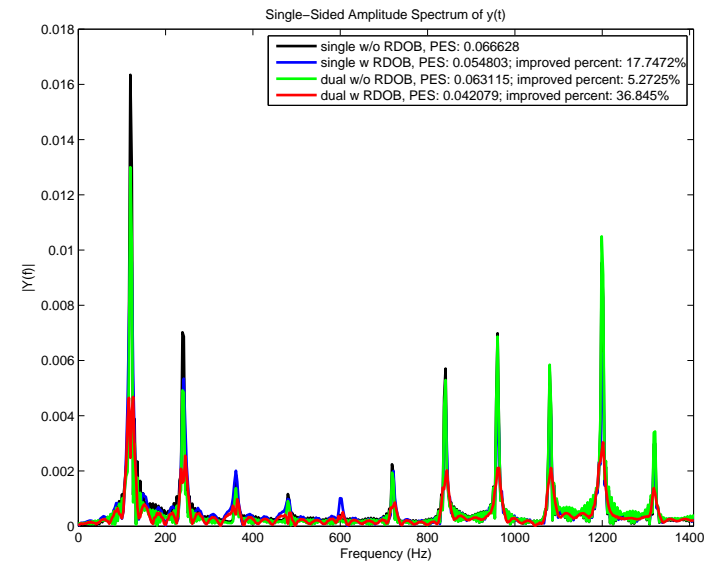
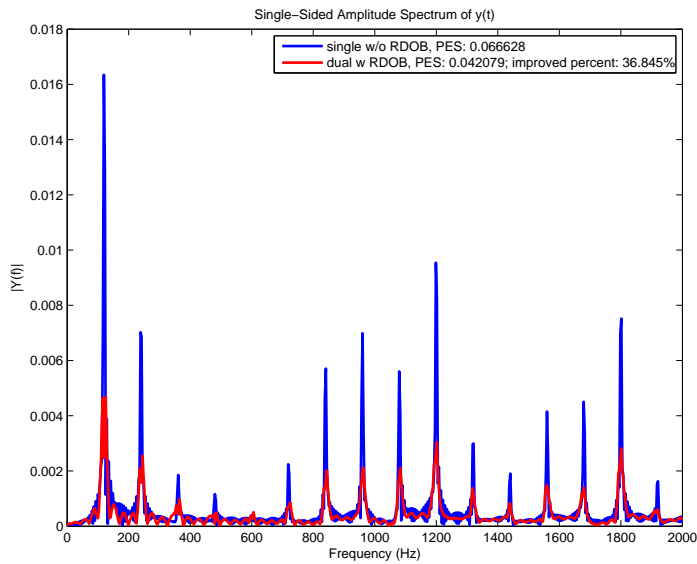


Figure 16: sensitivity function with Discrete LQG/LTR controller and RDOB for PZT loop only. Can see that due to the addition of bandpass filter, the selective band is only restricted to $720\text{--}3600\text{ Hz}$ for PZT loop RDOB. Thus PZT won't be used in unnecessary range.



(a) Single stage HDD with only repetitive disturbance, comparison between with and without RDOB

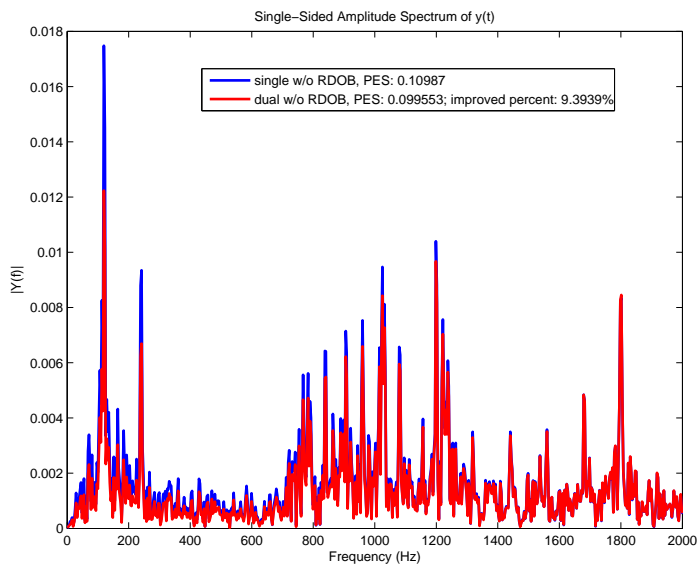
(b) HDDs with only repetitive disturbance, comparison between single stage and dual stage without RDOB



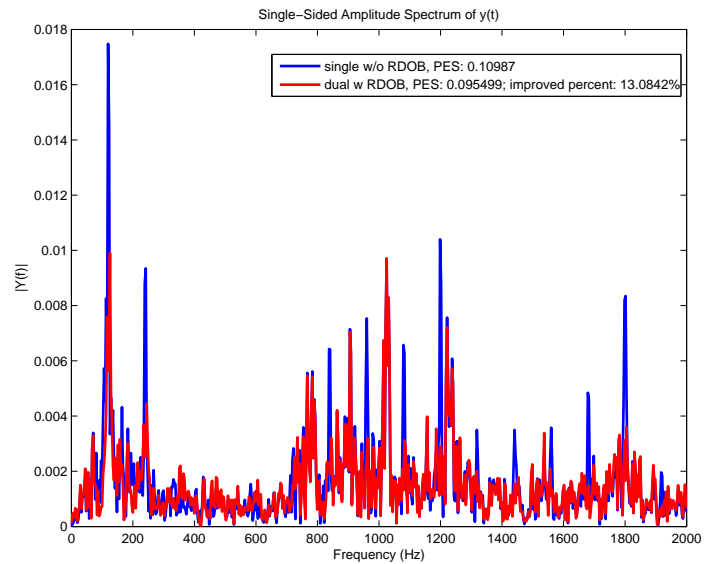
(c) HDDs with only repetitive disturbance, comparison between single stage and dual stage with RDOB

(d) HDDs with only repetitive disturbance, comparison between all the 3 cases

Figure 17: HDD servo with only repetitive disturbance. Compensation results between single stage and dual stage, with and without RDOB cases.



(a) HDDs with all disturbance, comparison between single stage and dual stage without RDOB



(b) HDD servo with repetitive and all other types of disturbance. Comparison result between single stage no RDOB and dual stage with RDOB

Figure 18: HDD servo with all disturbance. Compensation results between single stage and dual stage, with and without RDOB cases.

References

- [1] M. Athans. A tutorial on the lqg/ltr method. In *American Control Conference, 1986*, pages 1289–1296, June 1986.
- [2] X. Chen and M. Tomizuka. Decoupled disturbance observers for dual-input-single-output systems with application to vibration rejection in dual-stage hard disk drives. In *ASME 2012 5th Annual Dynamic Systems and Control Conference joint with the JSME 2012 11th Motion and Vibration Conference*, pages 619–628. American Society of Mechanical Engineers, 2012.
- [3] X. Chen and M. Tomizuka. New repetitive control with improved steady-state performance and accelerated transient. *Control Systems Technology, IEEE Transactions on*, 22(2):664–675, March 2014.
- [4] L. Guo, D. Martin, and D. Brunnett. Dual-stage actuator servo control for high density disk drives. In *Advanced Intelligent Mechatronics, 1999. Proceedings. 1999 IEEE/ASME International Conference on*, pages 132–137, 1999.
- [5] J. Maciejowski. Asymptotic recovery for discrete-time systems. *Automatic Control, IEEE Transactions on*, 30(6):602–605, Jun 1985.
- [6] A. A. Mamun and G. Guo. *Hard disk drive (mechatronics and control)*. CRC press, 2007.
- [7] G. Stein and M. Athans. The lqg/ltr procedure for multivariable feedback control design. *Automatic Control, IEEE Transactions on*, 32(2):105–114, Feb 1987.
- [8] M. Tomizuka. Dealing with periodic disturbances in controls of mechanical systems. *Annual Reviews in Control*, 32(2):193 – 199, 2008.